Available online at www.sciencedirect.com

ScienceDirect

European Journal of Protistology 54 (2016) 59–73

European Journal of PROTISTOLOGY

www.elsevier.com/locate/ejop

Description of two marine amphisiellid ciliates, *Amphisiella milnei* (Kahl, 1932) Horváth, 1950 and *A. sinica* sp. nov. (Ciliophora: Hypotrichia), with notes on their ontogenesis and SSU rDNA-based phylogeny

Liqiong Li[a,b,1], Xiaolu Zhao[a,1], Daode Ji[c], Xiaozhong Hu[a,d,*], Khaled A.S. Al-Rasheid[e], Saleh A. Al-Farraj[e], Weibo Song[a,d]

[a] *Institute of Evolution & Marine Biodiversity, Ocean University of China, Qingdao 266003, China*
[b] *School of Ocean, Yantai Academy, China Agricultural University, Yantai 264670, China*
[c] *School of Ocean, Yantai University, Yantai 264005, China*
[d] *Laboratory for Marine Biology and Biotechnology, Qingdao National Laboratory for Marine Science and Technology, China*
[e] *Zoology Department, King Saud University, Riyadh 11451, Saudi Arabia*

Received 19 August 2015; received in revised form 18 April 2016; accepted 18 April 2016
Available online 26 April 2016

Abstract

The morphology and taxonomy of two marine *Amphisiella* species, isolated from mariculture waters in northern China, were investigated using standard techniques. One species corresponds well with the original description of the poorly known *Amphisiella milnei* (Kahl, 1932) Horváth, 1950 by remarkable characteristics, inter alia, (i) the additional cirri between the left frontal cirrus and the buccal cirrus, and (ii) ring-shaped structure in the anterior and posterior body portion (posterior one sometimes lacking). The detailed description of the cirral pattern and an informative ontogenetic stage first reveal that the additional cirri, which are uniformly absent in all congeners, originate from the frontal-ventral transverse cirral anlage I. The other species represents a new species of *Amphisiella*, *A. sinica* sp. nov. It is distinguished from its most closely related congener *A. annulata* (Kahl, 1928) Borror, 1972 by having numerous ring-shaped structures with a shallow brim more or less densely centralised at both ends of the body. Brief notes on the cell division and phylogenetic analyses based on small subunit (SSU) rRNA gene sequence for both organisms are also supplied in order to get further understanding of their systematic positions. The molecular information indicates that both organisms belong to two separate clades and confirms that the genus *Amphisiella* might be polyphyletic.

Keywords: Infraciliature; *Amphisiella milnei*; *Amphisiella sinica* sp. nov.; New species; Amphisiellidae; SSU rDNA sequence

Introduction

Amphisiellids are a group of hypotrichous ciliates that are, inter alia, characterised by a more or less distinct frontoventral row, termed the amphisiellid median cirral row, which is derived from the two or three rightmost anlagen,

*Corresponding author at: Institute of Evolution & Marine Biodiversity, Ocean University of China, Qingdao 266003, China.
Tel.: +86 532 8203 1610.
E-mail address: xiaozhonghu@ouc.edu.cn (X. Hu).
[1] Contributed equally.

http://dx.doi.org/10.1016/j.ejop.2016.04.004
0932-4739/

and by forming their frontal-ventral-transverse cirri by six anlagen. So far ca. 60 nominal forms have been found, most of which live in terrestrial habitats, although some are marine (e.g. Berger and Foissner 1989; Blatterer and Foissner 1988; Dragesco 1963; Foissner et al. 2002; Gong et al. 2007; Gourret and Roeser 1888; Li et al. 2007a,b; Song and Wilbert 1997; Wilbert and Song 2005). Recently, Berger (2008) made a comprehensive revision of amphisiellids, and redefined the genus *Amphisiella* Gourret and Roeser, 1888 as follows: Amphisiellidae with continuous adoral zone of membranelles; undulating membranes straight and parallel; three enlarged frontal cirri; buccal cirrus present; two or more cirri left of anterior portion of the amphisiellid median cirral row, which originates from anlage V (posterior portion) and VI (anterior portion); postperistomial cirrus lacking; usually two pretransverse ventral cirri; five or more prominent transverse cirri; one left and one right marginal row; more than three dorsal kineties each originating intrakinetally; caudal cirri lacking; saltwater. According to this definition, only five species were included in the genus with *Amphisiella capitata* (Pereyaslawzewa, 1886) Borror, 1972 as the type, and *A. arenicola* Fernandez-Leborans and Novillo, 1992 was classified as an indeterminate species (Berger 2008; Fernandez-Leborans and Novillo 1992, 2001). Very recently, Chen et al. (2013) added two new species. Among these forms, three species, i.e. *Amphisiella ovalis* Fernandez-Leborans and Novillo, 1992, *A. turanica* Alekperov and Asadullayeva, 1999 and *A. milnei* (Kahl, 1932) Horváth, 1950 have not been described in detail in terms of their living features, infraciliature and/or morphogenesis (Alekperov and Asadullayeva 1999; Fernandez-Leborans and Novillo 1992; Horváth 1950; Kahl 1932) and 18S rRNA gene sequence data are unavailable for these three species yet (Chen et al. 2013). During a survey of the marine ciliate fauna in northern China, two organisms were isolated and studied using standard methods. One species was demonstrated to be conspecific with *Amphisiella milnei*. The other represents an unknown species. In addition, small subunit (SSU) rRNA gene sequence data and one ontogenetic stage were obtained for each species.

Material and Methods

Amphisiella sinica sp. nov. and *A. milnei* were collected from coastal waters off Qingdao (36°03′36″ N; 120°18′54″ E and 36°06′58″ N; 120°43′96″ E), China, on September 28th, 2007 (salinity 29‰, water temperature 24 °C, pH 8.0), and on October 24th, 2007 (salinity 30‰, water temperature 18 °C, pH 7.9), respectively. The ciliates were collected using microscope slides as artificial substrates that were fixed to a frame and immersed in the water at a depth of ca. 1 m for about one week to allow colonisation to occur (Lu et al. 2014). Following retrieval of the slides, ciliates were isolated and raw cultures were established at room temperature (24 °C) in Petri dishes containing filtered marine water with squeezed rice grains to enrich the bacterial food.

Ciliates were examined with bright field and differential interference contrast microscopy. The protargol silver staining method according to Wilbert (1975) was used to reveal the infraciliature. Measurements were carried out with an ocular micrometre. All drawings were performed at a magnification of 1250× with the aid of a camera lucida. To illustrate the changes occurring during the ontogenetic process parental cirri are depicted by contour whereas new ones are shaded black. Terminology is mainly according to Berger (2008).

Cells were washed several times by sterile seawater to remove other protists before the extraction of DNA. Genomic DNA was extracted according to the protocol for the REDExtract-N-Amp Tissue PCR Kit (Sigma, St. Louis, USA) as described by Fan et al. (2014). The universal primers Euk A (5′-AACCTGGTTGATCCTGCCAGT-3′) and Euk B (5′-TGATCCTTCTGCAGGTTCACCTAC-3′) (Medlin et al. 1988) were used for the SSU rRNA gene amplification. Running cycles of the Polymerase chain reaction (PCR) amplifications of the SSU rRNA gene were as follows: 5 min at 94 °C for initial denaturation, followed by 35 cycles of 94 °C for 30 s, 54 °C for 1 min, 72 °C for 2 min; the final extension was 10 min at 72 °C. The purifying, cloning and sequencing of the PCR products were performed according to Chen et al. (2015b). Primers used for sequencing were M13-47, M13-48 and two internal primers 900F (5′-CGATCAGATACCGTCCTAGT-3′) and 900R (5′-ACTAGGACGGTATCTGATCG-3′).

As revealed by Chen et al. (2013), the SSU rRNA gene sequence of *Amphisiella milnei* with the accession number DQ845293 could come from a misidentified population and thus was not used in the current phylogenetic analyses. Two new SSU rRNA gene sequences of *Amphisiella sinica* sp. nov. and *A. milnei* as well as 42 sequences of other species from the GenBank database were analysed. A total of 44 sequences were aligned using the online server GUIDANCE with the alignment algorithm MUSCLE (Penn et al. 2010a,b) provided on the web, and the automated removal of unreliable columns was performed with default parameters (below 0.93). Gblocks v0.91b (Castresana 2000) was used to remove the ambiguous blocks, resulting in an alignment of 1701 characters. The sequence identity matrix of species in the genus *Amphisiella* was performed using BioEdit 7.0.0 (Hall 1999).

Ciliates in Phacodiniidia and Protocruziidia were chosen as the out-group species. Maximum likelihood (ML) analyses were conducted using the tool kit RAxML-HPC2 on XSEDE v 7.2.8 (Stamatakis 2006; Stamatakis et al. 2008), which was implemented in the online server CIPRES Science Gateway (Miller et al. 2010) using the GTR + G model. The reliability of internal branches was estimated by bootstrapping with 1000 replicates. Bayesian inference (BI) analysis was performed using MrBayes on XSEDE v 3.1.2 (Ronquist and Huelsenbeck 2003) on CIPRES Science Gateway with the GTR + G model, chosen under the Akaike Information (AI) Criterion in MrModeltest v2 (Nylander 2004). Markov chain Monte Carlo (MCMC) simulations were then run with two sets of four chains using the default settings of a chain

length of 2,000,000 generations and trees sampled every 100 generations. The first 25% of sampled trees were discarded as burn-in. The posterior probabilities (PP) were calculated from the remaining trees using a majority rule consensus. MEGA 5 (Kumar et al. 2008) was used to visualise tree topologies.

Results

Amphisiella milnei (Kahl, 1932) Horváth, 1950 (Figs 1–3 and Table 1)

Basionym: *Holosticha* (*Amphisiella*) *milnei* Kahl, 1932.

Since the first reports by Kahl (1932, 1933), this species was found on several occasions but no more details have been provided (Agamaliev 1972; Aladro-Lubel et al. 1986; Berger 2008). Furthermore, details of the infraciliature are unknown yet. Our organism corresponds well with the original description of *Amphisiella milnei* in live features (e.g. cell shape and size, cortical granules, ring-shaped structures, two macronuclear nodules) and cirral arrangement, and thus both are very likely conspecific. Here we present an improved diagnosis based on all available data and a detailed description of the Chinese population.

Improved diagnosis

Size in vivo about 100–160 × 20–40 μm. Body elongate elliptical, dark yellowish to slightly brownish in colour at low magnification. Fine, light yellowish coloured cortical granules irregularly and densely distributed ventrally, while grouped in longitudinal stripes dorsally. Usually one large ring-shaped structure at each end of body. 27–43 adoral membranelles and 23–37 right and 27–39 left marginal cirri. Three frontal cirri, usually two cirri behind left frontal cirrus, one buccal cirrus, one parabuccal cirrus; consistently three frontoventral cirri, two pretransverse ventral cirri, and about five transverse cirri; seven bipolar dorsal kineties. Amphisiellid median cirral row shortened posteriorly and composed of 22–36 cirri; two macronuclear nodules. Marine and brackish habitats.

Deposition of voucher slides

One protargol preparation slide was deposited in the Laboratory of Protozoology, Ocean University of China with registration number LLQ-20070928-02. A second slide was deposited in the Natural History Museum, London (registration number: NHMUK 2010:1:30:3).

Morphological description of Chinese population

Cell size about 110–160 × 30–40 μm in vivo; body usually elongate-elliptical in outline; both ends widely rounded, margins more or less straight depending on feeding situation (Figs 1A, B, 2A, E). Living cells seem dark yellowish to slightly brownish in colour at low magnification. Body flexible and inconspicuously contractile, dorsoventrally flattened about 3:1 (Fig. 2D). Ventral side flat with three indistinctive grooves along marginal rows and amphisiellid median cirral row (Fig. 2D, E, L). Cytoplasm colourless to greyish, often filled with many shining globules (3–5 μm in diameter). Pellicle comparatively thick, with light yellowish cortical granules (about 0.5 μm across), which are irregularly densely distributed ventrally, while grouped in longitudinal stripes throughout whole dorsal side (Figs 1H, 2F, G, K, L). Usually one hollow sphere (ring-shaped structure), 6–7 μm in diameter, conspicuously appears in anterior and posterior portions of body (Figs 1A, E, 2A, I). Posterior sphere sometimes lacking or situated in mid-body portion (Fig. 1B). Contractile vacuole not observed, possibly lacking. Two ellipsoidal macronuclear nodules, on average 17 × 10 μm in size, positioned slightly left of midline, roughly in central body portion, transparent and detectable in vivo even with bright field microscopy at low magnification (Figs 1A, B, D, 2B, C, J, 3A). Two to five, mostly three, micronuclei adjacent to macronuclear nodules (Fig. 1D). Locomotion moderately slow. Individuals crawl on bottom of Petri dish or on debris, with short and frequent pauses and intermittently change their direction.

Buccal field dominant; adoral zone occupying about 30–40% of body length, with its distal end extending posteriorly to about one quarter of buccal field (Figs 1A–C, F, 2C, E). Base of the membranelles in proximal portion around 8 μm wide. Undulating membranes probably roughly straight and side by side; paroral slightly in front of endoral (Figs 1C, 3C). Three slightly enlarged frontal cirri in oblique pseudorow along distal portion of adoral zone, while parabuccal cirrus (= cirrus III/2) located left behind right frontal cirrus (Figs 1A, C, F, 2H, 3C, D). One buccal cirrus positioned at right of anterior third of undulating membranes (Figs 1C, F, 3C). Usually two, rarely one or three cirri (5 specimens out of 25) behind left frontal cirrus longitudinally situated above buccal cirrus (Figs 1A, 2H, 3C). Amphisiellid median cirral row (ACR) composed of 22–36 cirri, mostly grouped in two inconspicuous segments, extends from distal end of adoral zone to about posterior 75% of cell. All cirri in ACR of equal size (Figs 1C, F, 3B). Consistently, three frontoventral cirri positioned left of anterior portion of ACR (Figs 1C, 3D). Five, very rarely four, slightly enlarged transverse cirri, arranged in a J-shaped pseudorow, with cilia projecting three-quarters of their length beyond posterior body margin in live specimens. Two fine pretransverse ventral cirri closely located above right two transverse cirri (Figs 1C, 3E). Right marginal row commencing above level of proximal end of adoral zone, ending sub-terminally and therefore distinctly separated from rear end of left marginal row, which commences to left of proximal portion of adoral zone (Figs 1C, F, 3A). Six almost bipolar dorsal kineties, bristles around 3 μm long. Caudal cirri obviously lacking (Fig. 1C, D).

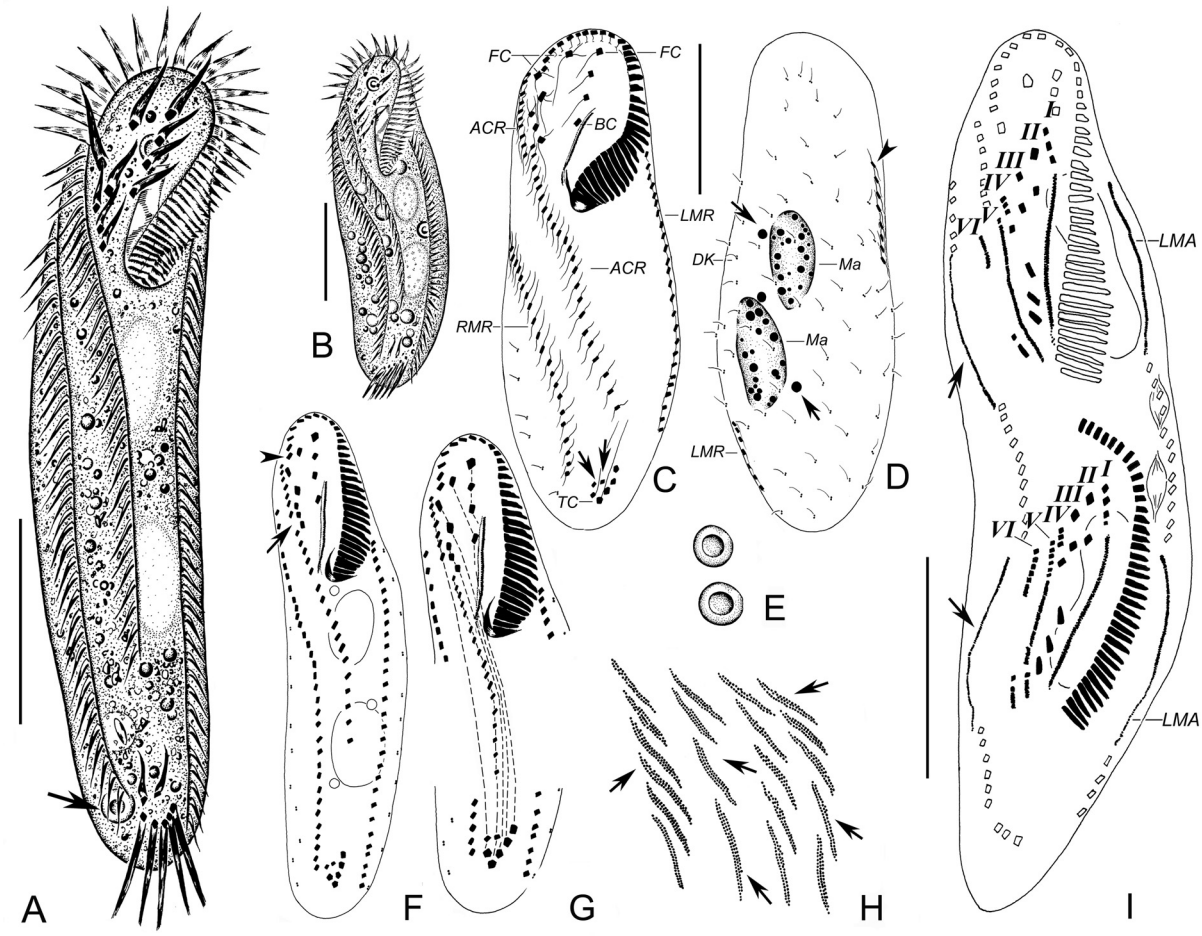

Fig. 1. (A–I) Morphology of *Amphisiella milnei* from life (A, B, E, H) and after protargol staining (C, D, F, G, I). (A) Ventral side of a representative specimen; arrow marks the ring-shaped structure. (B) To show the different body shape. (C, D) Ventral and dorsal side of the same specimen to show the infraciliature and nuclei, arrows in (C) indicate the fine pretransverse ventral cirri, arrows and arrowhead in (D) mark the micronuclei and the anterior portion of right marginal row respectively. (E) Ring-shaped structures. (F) Infraciliature on ventral side of another specimen, arrowhead depicts membranelle at distal end of adoral zone and arrow indicates the gap in the amphisiellid medium cirral row. (G) Ventral side, to demonstrate the development of cirri, broken line connects cirri originating from the same anlage. (H) Dorsal side, arrows mark the grouped tiny cortical granules. (I) Ventral side of a middle divider, arrows mark the right marginal row anlagen. ACR, amphisiellid median cirral row; BC, buccal cirrus; DK, dorsal kineties; FC, frontal cirri; I–VI, frontal-ventral-transverse cirral anlagen I–VI; LMA, left marginal row anlagen; LMR, left marginal row; Ma, macronuclear nodule; RMR, right marginal row; TC, transverse cirri. Scale bars = 30 μm.

Notes on morphogenesis

Only one middle divider was observed (Figs 1I, 3H). The following phenomena can be deduced: (1) the parental adoral zone of membranelles is very likely completely inherited by the proter; (2) the marginal row anlagen develop within the parental structures; (3) the frontal-ventral-transverse cirri originate from six cirral anlagen: anlage I (= undulating membrane anlage) → undulating membranes (paroral membrane, endoral membrane), left frontal cirrus, cirri behind left frontal cirrus; anlage II → middle frontal cirrus, buccal cirrus, left transverse cirrus; anlage III → right frontal cirrus and parabuccal cirrus (cirrus III/2), second transverse cirrus from left; anlage IV → three frontoventral cirri left of anterior portion of ACR, third transverse cirrus from left; anlage V → fourth transverse cirrus from left, left pretransverse ventral cirrus, and posterior part of ACR; anlage VI → fifth transverse cirrus from left, right pretransverse ventral cirrus, and anterior portion of the ACR (Figs 1G, I, 3H).

Amphisiella sinica sp. nov. (Figs 4–6, Table 1)

Diagnosis

Size in vivo about 135–180 × 30–40 μm. Body elongate elliptical to fusiform with anterior portion distinctly cephalised and curved leftwards. Two macronuclear nodules. Two kinds of colourless cortical granules: larger ones grouped along dorsal kineties; smaller ones distributed in whole cortex. Ring-shaped structures with shallow brim,

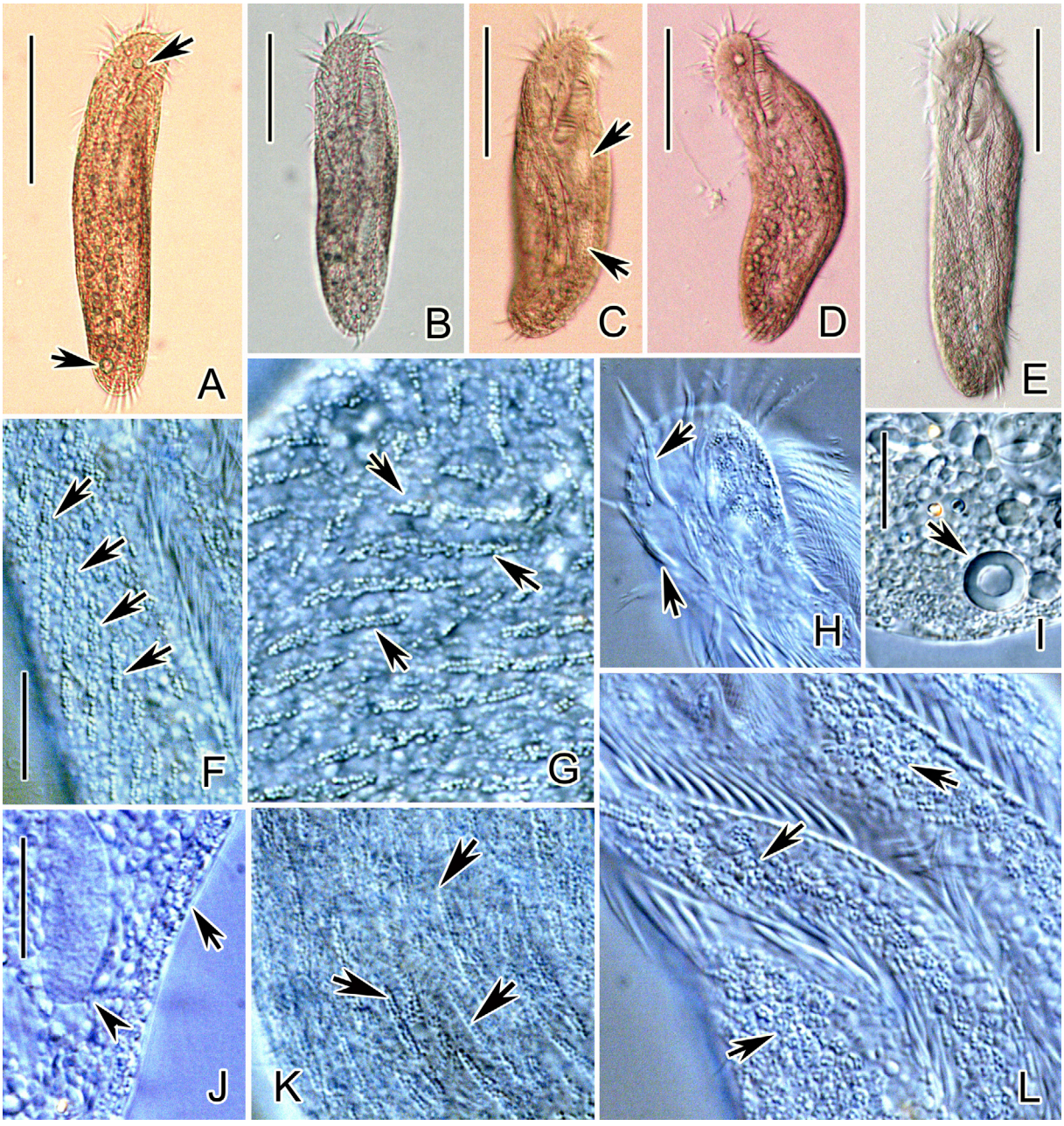

Fig. 2. (A–L) Photomicrographs of *Amphisiella milnei* from life. (A, E) Ventral side of representative specimens, arrows in (A) depict the ring-shaped structures. (B, C) Ventral side of specimens to show different body shapes, arrows indicate the macronuclear nodules. (D) Ventral side, to show the flexibility of the body. (F) Ventral side, arrows indicate the cortical granules grouped in streaks. (G, K) Dorsal side, arrows mark the tiny cortical granules. (H) Ventral side of oral field, arrows indicate the slightly enlarged middle and right frontal cirrus. (I) Ring-shaped structure in the rear end of body (arrow). (J) Lateral view of partial body, to demonstrate the thick cortex (arrow) and macronuclear nodule (arrowhead). (L) Ventral side of middle portion of the specimen, to show the shallow grooves with the cirral rows and the tiny cortical granules (arrows). Scale bars: A–E = 50 μm, F, I, J = 10 μm.

more or less densely centralised in anterior and posterior body portions. Amphisiellid median cirral row extending to transverse cirri, and consisting of about 47 narrowly spaced cirri. On average 55 adoral membranelles. Left and right marginal row composed of 33–44 and 31–49 cirri, respectively. Consistently three slightly enlarged frontal cirri, one buccal cirrus, one parabuccal cirrus, three cirri left of anterior portion of amphisiellid median cirral row, two pretransverse ventral cirri, usually six transverse cirri, and six dorsal kineties. Marine habitat.

Type locality

Seawater near the pontoon bridge of Zhanqiao Pier at Qingdao (36°03′36″ N; 120°18′54″ E), China.

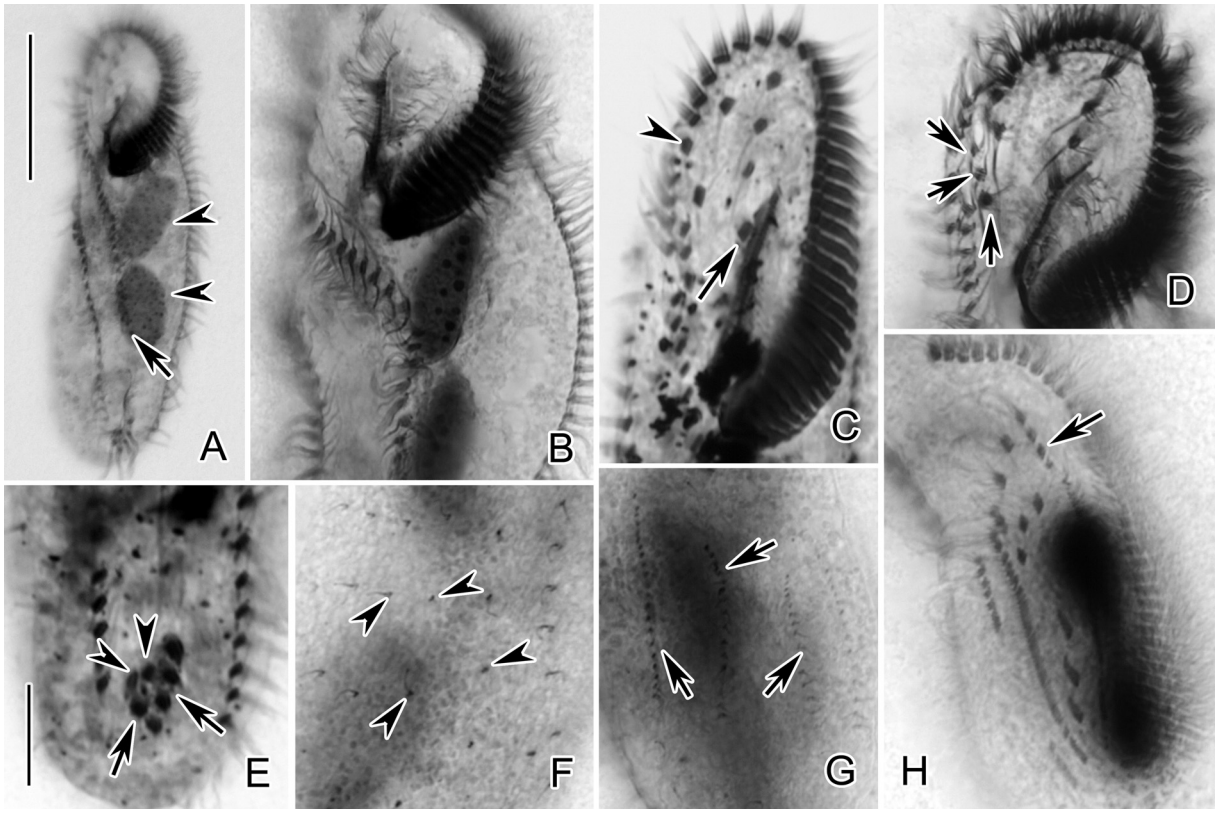

Fig. 3. (A–H) Photomicrographs of *Amphisiella milnei* after protargol staining. (A) Ventral side, to show the infraciliature and macronuclear nodules (arrowheads), arrow indicates amphisiellid medium cirral row. (B) Ventral side of the anterior and middle portion of a specimen, to show the amphisiellid medium cirral row. (C) Ventral side of the anterior portion of body, arrow indicates the buccal cirrus, arrowhead marks the right frontal cirrus close to the distal end of the adoral zone of membranelles. (D) Part of the buccal field, arrows indicate the frontoventral cirri. (E) Ventral side of the cell end to show the fine pretransverse ventral cirri (arrowheads) and the transverse cirri (arrows). (F) Dorsal side, arrowheads indicate the dorsal kineties. (G, H) Dorsal (G) and ventral (H) side of the same middle divider, arrows in (G) and arrow in (H) showing the dorsal kineties anlagen and the new cirri generated from the undulating membranes anlage, respectively. Scale bars: A = 40 μm, E = 10 μm.

Type slides

One slide of protargol-impregnated specimens including the holotype (Fig. 4F, G) was deposited in the Laboratory of Protozoology, Ocean University of China with registration number LLQ-20071024-01. A second slide with paratypes was deposited in the Natural History Museum, London (registration number: NHMUK 2010:1:30:4).

Etymology

The species-group name *sinica* (Latin; Chinese) refers to the country (China) where the species was discovered.

Morphological description

Live specimens usually about 135–180 × 30–40 μm in size, ratio of length to width ranging between 5:1 and 4:1; body outline elongate elliptical to slightly fusiform, with conspicuously cephalised and leftwards curved anterior portion and rounded posterior end. Left margin more convex than right one (Figs 4A, B, F, 5A, D). Body soft, flexible, and often slightly twisted about main axis, not distinctly contractile (Fig. 5C, D). Ventral side slightly uneven with three furrows along marginal and amphisiellid median cirral rows, which can be easily detected in living cells (Fig. 5B, C). Invariably two ellipsoidal macronuclear nodules slightly left of midline; individual nodules in life up to about 30 × 10 μm. Micronuclei ellipsoidal and adjacent to macronuclear nodules (Figs 4A, G, 6C, F). Two kinds of colourless cortical granules: larger granules globular, about 1.0 μm across, grouped along dorsal kineties; some subconically shaped and 4–5 μm long when ejected (Figs 4E, 5J, 6E); smaller ones about 0.3–0.5 μm across and more or less densely distributed in whole cortex (Figs 4E, 5E, F, J). Cytoplasm colourless, contains about 70–100 ring-shaped structures (lithosomes?), 4–5 μm in diameter, with fine and shallow brim, basically arranged densely in anterior and posterior portion, render body opaque and greyish in colour under low magnification (Figs 4B, D, 5A, G–I). Several conspicuous food vacuoles, up to about 15 μm across, very probably containing diatoms and bacteria, scattered mainly within cell centre. Locomotion moderately rapid. Individuals crawl on bottom of Petri dish or on debris, with short and frequent pauses and intermittently change their direction.

Table 1. Morphometric data of *Amphisiella milnei* (first line) and *A. sinica* sp. nov. (second line). Data based on protargol-impregnated specimens.

Character	Min	Max	Mean	Median	SD	CV	SE	*n*
Length of body (μm)	92	144	113.4	112	13.5	11.9	2.7	25
	130	180	159.7	160	14.6	9.1	2.9	25
Width of body (μm)	32	48	38.9	38	4.2	10.7	0.8	25
	22	48	34.9	34	6.1	17.4	1.2	25
Length of adoral zone (μm)	28	48	39.0	40	4.8	12.3	1.0	25
	50	76	64.9	66	6.1	9.3	1.2	25
Number of adoral membranelles	27	43	37.5	38	4.0	10.6	0.8	25
	46	64	54.9	55	4.6	8.3	0.9	25
Number of buccal cirri	1	1	1	1	0	0	0	25
	1	1	1	1	0	0	0	25
Number of frontal cirri	3	3	3.0	3	0	0	0	25
	3	3	3.0	3	0	0	0	25
Number of cirri behind left frontal cirrus	1	3	2.0	2	0.4	17.9	0.1	25
	0	0	0	0	0	0	0	25
Number of parabuccal cirri	1	1	1	1	0	0	0	25
	0	1	1.0	1	0.2	20.8	0	25
Number of frontoventral cirri	3	3	3	3	0	0	0	25
	3	3	3	3	0	0	0	25
Number of cirri in amphisiellid median cirral row	22	36	29.9	30	3.6	12.0	0.7	25
	41	52	46.8	47	2.7	5.8	0.5	25
Number of left marginal cirri	27	39	33.8	34	3.0	8.9	0.6	25
	30	44	38.1	38	3.2	8.5	0.6	25
Number of right marginal cirri	23	37	32.2	33	3.2	9.9	0.6	25
	31	49	39.1	39	4.2	10.8	0.8	25
Number of pretransverse ventral cirri	2	2	2	2	0	0	0	25
	2	2	2	2	0	0	0	25
Number of transverse cirri	4	5	5.0	5	0.2	4.0	0	25
	6	7	6.1	6	0.3	5.4	0.1	25
Number of dorsal kineties	7	7	7	7	0	0	0	25
	6	6	6	6	0	0	0	25
Number of macronuclear nodules	2	2	2	2	0	0	0	25
	2	2	2	2	0	0	0	25
Number of micronuclei	2	5	2.6	2	0.8	30.0	0.2	25
	2	8	4.2	4	1.6	37.0	0.3	25
Length of macronuclear nodule (μm)	12	24	17.0	18	2.5	14.5	0.5	25
	14	30	21.5	22	3.9	18.3	0.8	25
Width of macronuclear nodule (μm)	8	12	9.6	10	1.3	13.1	0.3	25
	5	14	9.6	8	3.1	32.4	0.6	25

Abbreviations: CV, coefficient of variation in %; Max, maximum; Mean, arithmetic mean; Median, median value; Min, minimum; *n*, number of specimens analysed; SD, standard deviation; SE, standard error.

Buccal field narrow, about 1/3 of body width. Adoral zone comprising 55 membranelles on average, and occupying 37–48% of body length, proximal portion usually slightly spoon-shaped (Figs 4A, B, 5A, D, 6C). Distal end of adoral zone extending on to 12% of body length on right body margin (Figs 4C, 5A). Undulating membranes arranged straight and in parallel; 2-rowed paroral membrane longer than single-rowed endoral membrane, and ahead of latter (Fig. 4C). Cirral pattern and number of cirri show usual variability (Table 1). Three distinctly enlarged frontal cirri in oblique pseudorow along distal portion of adoral zone, while parabuccal cirrus (= cirrus III/2) located left behind right frontal cirrus (Figs 4C, F, 6H). One buccal cirrus (= cirrus II/2) of same size as frontal cirri, situated right of anterior end of paroral membrane (Figs 4C, 6H). ACR composed of 47 cirri on average, commences to the right frontal cirrus and terminates posteriorly ahead of transverse cirri. Cirri within ACR narrowly spaced, especially in middle part where they are also rather wide, that is, up to 4–5 μm (Figs 4F, 6D). A row of three frontoventral cirri present to left of anterior portion of ACR (Figs 1C, 6H). Usually six, rarely seven (3 out of 25 specimens) transverse cirri arranged in J-shaped and slightly subterminal pseudorow; cirri about 15 μm long in life and distinctly projecting beyond rear body end (Figs 4F, 6I). Consistently two rather fine pretransverse ventral cirri: right one ahead of rightmost transverse cirrus; and left one behind

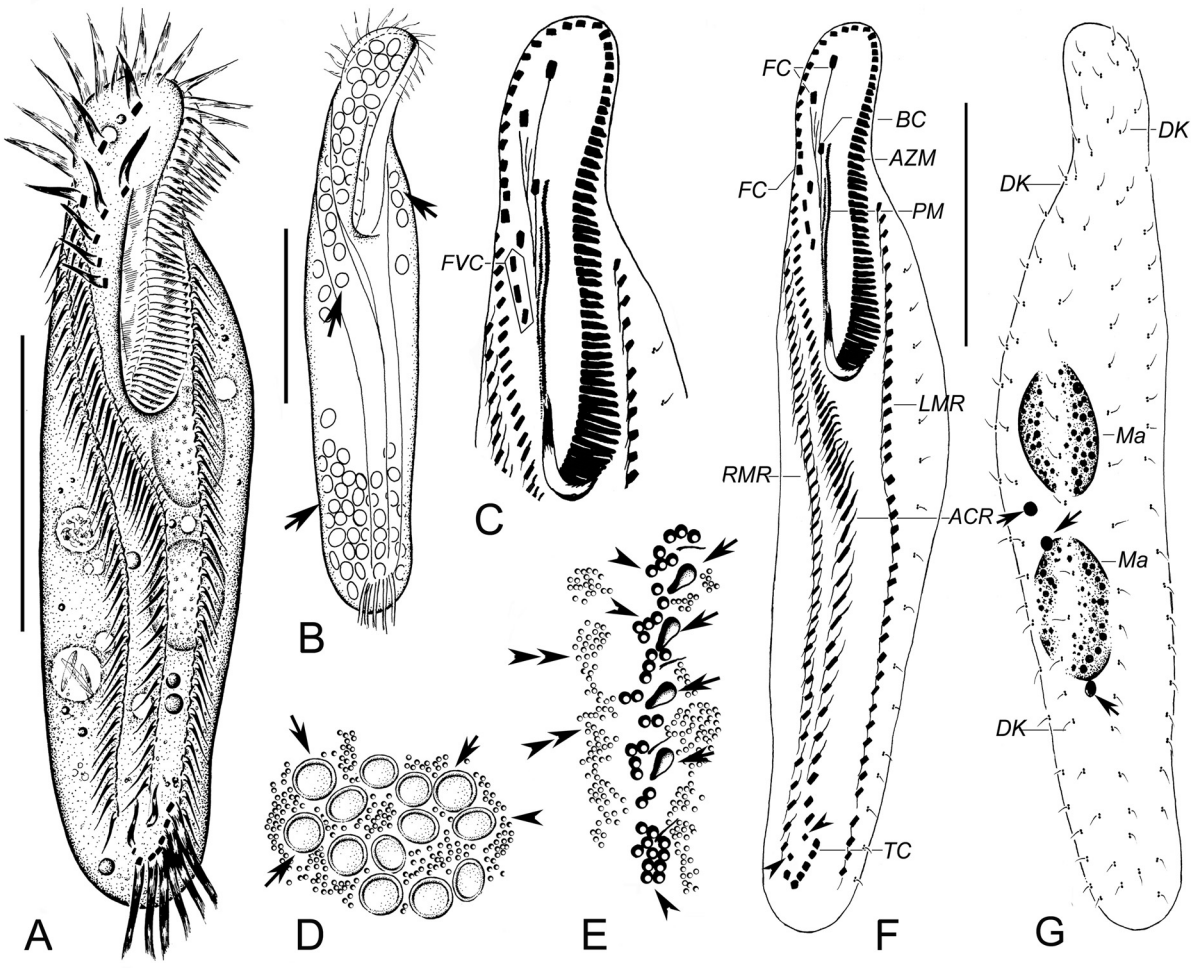

Fig. 4. (A–G) Morphology of *Amphisiella sinica* sp. nov. from life (A, B, D, E) and after protargol staining (C, F, G). (A) Ventral side of a representative specimen. (B) Ventral side to show the number and arrangement of the ring-shaped structures (arrows). (C) Ventral side of the anterior portion of a specimen, showing frontal ciliature and oral apparatus. (D) Ring-shaped structures (arrows) and tiny dot-like granules (arrowhead). (E) Part of dorsal cortex, arrows indicate the ejected cortical granules, arrowheads mark the larger cortical granules, double-arrowheads indicate the tiny dot-like granules. (F, G) Ventral (F) and dorsal (G) side of the holotype specimen to show the infraciliature and nuclear apparatus, arrowheads indicate the fine pretransverse ventral cirri, arrows mark the micronuclei. ACR, amphisiellid median cirral row; AZM, adoral zone of membranelles; BC, buccal cirrus; DK, dorsal kineties; FC, frontal cirri; FVC, frontoventral ciri; LMR, left marginal row; Ma, macronuclear nodules; PM, paroral membrane; RMR, right marginal row; TC, transverse cirri. Scale bars: A, C = 50 μm, F, G = 45 μm, D, E = 10 μm.

posterior end of ACR and near leftmost transverse cirrus (Figs 4F, 6I). Marginal cirri relatively narrowly spaced and about 8 μm long in life. Left marginal row commencing at level of mid-buccal field, and ending subterminally; right marginal row beginning at anterior quarter of body and terminating near right pretransverse ventral cirrus (Figs 4F, 6C, I). Six more or less bipolar dorsal kineties consistently present, with about 3 μm long dorsal cilia (Figs 4G, 6E).

Notes on morphogenesis

Only one mid-late divider was found (Fig. 6A, B, G), revealing the following morphogenetic features: (1) the frontal-ventral-transverse cirri originate from basically six cirral anlagen (I–VI): anlage I (= undulating membrane anlage) → left frontal cirrus (= cirrus I/1), and undulating membranes (paroral, endoral); anlage II → middle frontal cirrus (= cirrus II/3), buccal cirrus (= cirrus II/2), and left transverse cirrus (= cirrus II/1); anlage III → second transverse cirrus from left (= cirrus III/1), parabuccal cirrus (= cirrus III/2), and right frontal cirrus (= cirrus III/3); anlage IV → third transverse cirrus from left (= cirrus IV/1) and three frontoventral cirri left of anterior portion of ACR; anlage V → fifth transverse cirrus from left (= cirrus V/1), left pretransverse ventral cirrus (= cirrus V/2), and posterior portion of the ACR; anlage VI → sixth transverse cirrus from left (= cirrus VI/1), right pretransverse ventral cirrus (= cirrus VI/2), and anterior portion of the ACR; (2) the parental adoral zone of membranelles remains more or less unchanged; (3) the anlagen of marginal rows and dorsal kineties occur within the parental structures. No caudal cirri

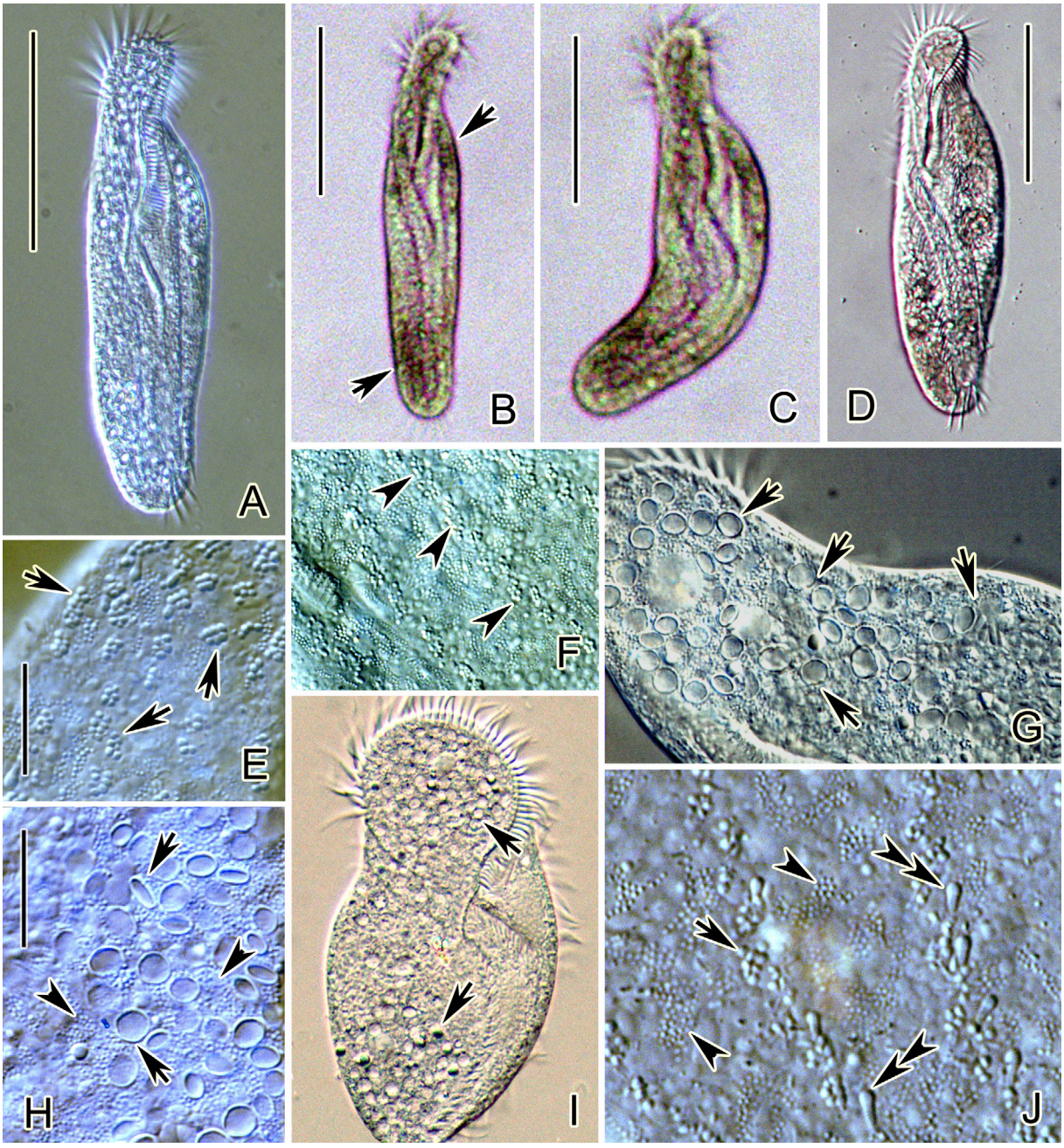

Fig. 5. (A–J) Photomicrographs of *Amphisiella sinica* sp. nov. from life. (A) Ventral side of a representative specimen. (B, D) Ventral side of two specimens to show variation of body shapes, arrows note the opacity caused by the ring-structures. (C) Ventral side, to show the flexibility of the body. (E) Dorsal side of anterior portion, arrows indicate the larger cortical granules. (F) Dorsal side, arrowheads indicate the cortical granules grouped along the dorsal kineties. (G, H) Arrows indicate the ring-shaped structures within the cytoplasm, arrowheads in (H) mark the tiny granules. (I) Ventral side of a squeezed specimen to demonstrate the arrangement of ring-shaped structures (arrows). (J) Part of dorsal side showing the larger cortical granules (arrow), the tiny dot-like granules (arrowheads) and the ejected cortical granules (double-arrowheads). Scale bars: A–D = 70 μm, E, H = 20 μm.

are formed at rear ends of dorsal kineties anlagen. Additionally, another feature can be deduced according to the closely related congener *Amphisiella annulata*, that is, an additional cirral anlage between the ordinary anlagen IV and V often produces one extra cirrus (fourth transverse cirrus from left, rarely two) so that totally six transverse cirri are formed.

SSU rRNA gene sequence and phylogenetic analyses (Fig. 7 and Table 2)

The SSU rRNA gene sequence data of *Amphisiella milnei* and *A. sinica* sp. nov. have been deposited in GenBank with the accession numbers FJ870072 and FJ870073. The length

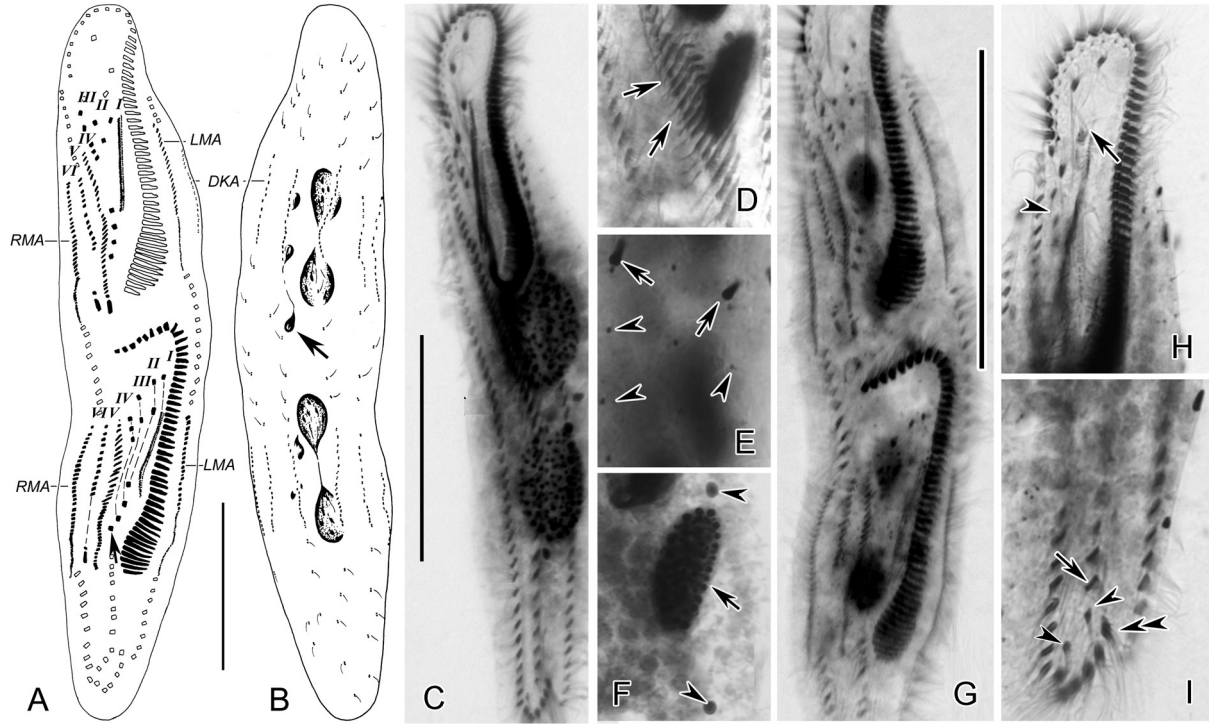

Fig. 6. (A–I) Divider (A, B, G) and interphasic specimens (C–F, H, I) of *Amphisiella sinica* sp. nov. after protargol staining. (A, G) Ventral side of the same mid-late divider, cirri originating from same anlage connected by broken line. Arrow marks the fourth transverse cirrus derived from an additional cirral anlage between anlagen IV and V. (B) Dorsal side of the same specimen as (A, G), arrow indicates the separating micronuclei. (C) Ventral side of the holotype, to show the infraciliature and nuclear apparatus. (D) Ventral side, arrow indicates the wide, narrowly spaced cirri with stained fibrils in the amphisiellid medium cirral row. (E) Dorsal side, to show extrusomes (arrows) and dorsal kineties (arrowheads). (F) To show the macronuclear nodule (arrow) and micronuclei (arrowheads). (H) Ventral side of anterior portion of body, arrowhead indicates the frontoventral cirri, arrow marks the buccal cirrus. (I) Ventral side of the cell end, to demonstrate the fine pretransverse ventral cirri (arrowheads), the posterior end of the amphisiellid medium cirral row (arrow) and the slightly enlarged transverse cirri (double-arrowhead). DKA, dorsal kineties anlagen; I–VI, frontal-ventral-transverse cirral anlagen I–VI; LMA, left marginal row anlagen; RMA, right marginal row anlagen. Scale bars: A, B = 40 μm, C, G = 50 μm.

Table 2. The structural similarities of the SSU rRNA gene sequences of *Amphisiella milnei*, *A. candida*, *A. sinica* sp. nov., *A. annulata*, and *A. pulchra*, determined according to Elwood et al. (1985).

	A. milnei	*A. candida*	*A. pulchra*	*A. sinica* sp. nov.
A. candida	0.988			
A. pulchra	0.955	0.957		
A. sinica sp. nov.	0.954	0.956	0.983	
A. annulata	0.955	0.957	0.992	0.983

and G + C content are 1772 bp, 45.43% for *Amphisiella milnei* and 1773 bp, 46.02% for *A. sinica* sp. nov., respectively. The SSU rRNA gene sequence similarities of species in the genus *Amphisiella* are in the range of 0.983–0.992 (Table 2).

Phylogenetic trees constructed by BI and ML methods generated nearly identical topologies. We therefore combined them into one consensus tree (Fig. 7). *Amphisiella sinica* sp. nov. clusters with two congeners, i.e. *A. annulata* and *A. pulchra* in a fully supported clade of the genus *Amphisiella* (group I), which is consistent with the morphological classification. *Amphisiella milnei* together with *A. candida* forms a distinctive clade (group II) from group I with relatively high support values (ML 99% BI 1.00).

Discussion

The new species *Amphisiella sinica* sp. nov.

In terms of body shape, general cirral pattern, two macronuclear nodules, the morphometric data and, especially, the two size classes of the cortical granules, the most closely related congener of the new species should be *A. annulata* (Kahl, 1928) Borror, 1972 that is rather recognisable by the wide and narrowly spaced cirri of the ACR, even in life, and the conspicuous ring-shaped structures. A significant difference between both in respect to the ring-shaped structures could not be ignored, however. For *A. annulata*,

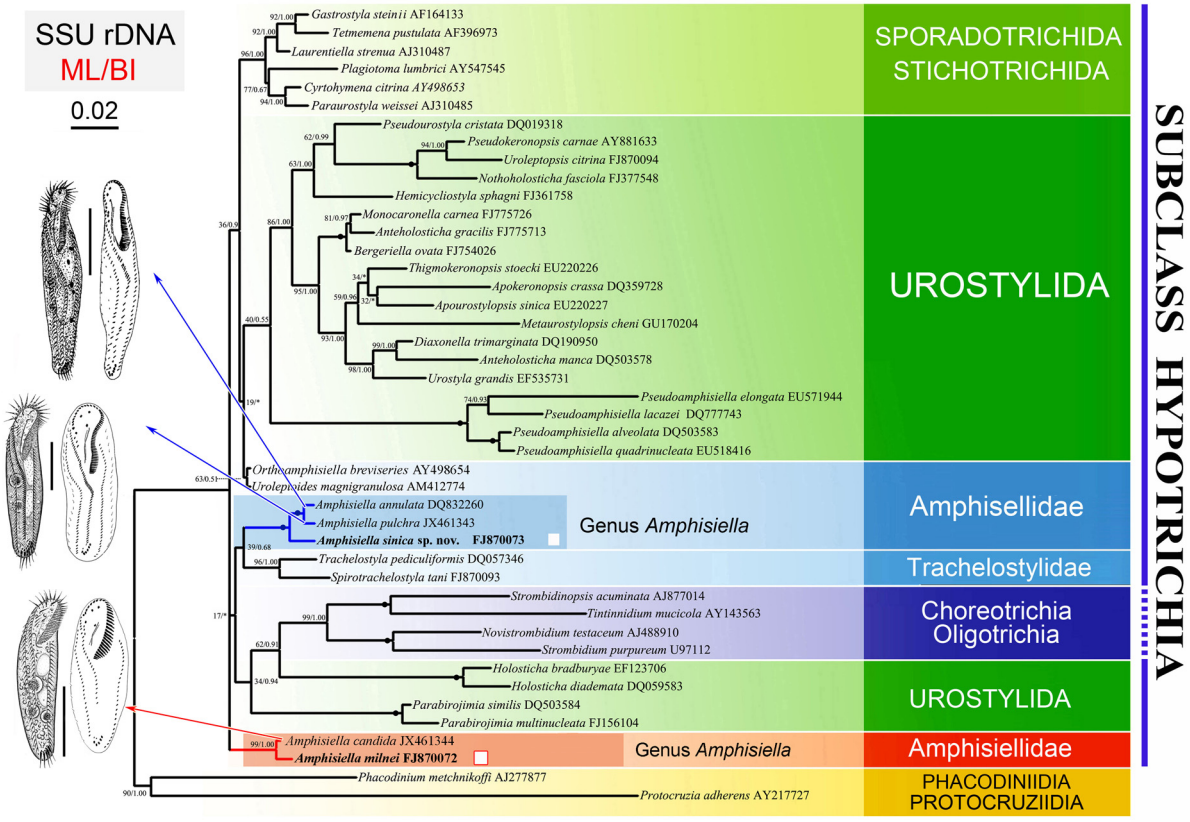

Fig. 7. Maximum likelihood (ML) phylogenetic tree based on the small subunit (SSU) rRNA gene sequences. Numbers at the nodes represent the bootstrap values of ML analyses and posterior probability of BI analyses. Fully supported (100%/1.00) branches are marked with solid circles. Asterisk (*) represents disagreement between BI and the reference ML tree. The scale bar corresponds to 2 substitutions per 100 nucleotide positions. Species newly sequenced in the present study are shown in bold. Inset figures from top to bottom cited from Hu et al. (2004) and Chen et al. (2013) to show the live morphology and infraciliature of *Amphisiella annulata*, *A. pulchra*, and *A. candida* respectively. Scale bars = 50 μm.

although some of the previous reports did not mention the ring-shaped structures, suggesting that these are sometimes lacking, nonetheless, the basic number and arrangement of this kind of organelle can be confirmed: that is, several (up to about 20 in the Adriatic neotype population), about 4–8 μm in diameter, sparsely distributed within endoplasm (Aladro-Lubel 1985; Alekperov and Asadullayeva 1999; Berger 2004; Borror 1963; Hu et al. 2004; Kahl 1928, 1932, 1933; Li et al. 2007a). In contrast, for *A. sinica* sp. nov., similar organelles are about 70–100 in number, 4–5 μm in diameter, with a fine and shallow brim, and basically arranged densely in the anterior and posterior portions of body. The new species has the paroral membrane located distinctly ahead of the endoral membrane and a distinctly cephalised anterior body end, while the neotype population of *A. annulata* possesses undulating membranes at almost the same level and a non-cephalised anterior body end (Berger 2004). But the Chinese population of *A. annulata* resembles the new species in these two aspects, so the conspecificity of both forms cannot be excluded to some extent (Hu et al. 2004). Furthermore, the molecular data evidently indicate that both forms should not be conspecific (30 bp difference) since SSU rDNA sequences among congeners in hypotrichs always exhibit very steady deviation as revealed in numerous recent studies (Chen et al. 2013; 2015a,b; Fan et al. 2014, 2015; Jo et al. 2015; Lu et al. 2014; Luo et al. 2015). So *A. annulata* and *A. sinica* sp. nov. should be distinct species.

Another closely related congener, *Amphisiella pulchra* Chen et al., 2013, is mainly distinguished from *A. sinica* sp. nov. by: (1) one type of cortical granules (vs. two types); (2) a slightly yellow-brownish body colour in life (vs. opaque and greyish); (3) the scattered ring-shaped structures (vs. densely arranged in both ends); (4) 7–9 dorsal kineties (vs. 6). Thus, these two forms cannot be confused (Chen et al. 2013).

As exhibited in Table 3, the new species can be distinguished from other congeners, the critical living features of which are available (*Amphisiella capitata*, *A. milnei*, *A. candida*) by having two types of cortical granules (vs. one type) and 70–100 ring-shaped structures (vs. absent or several in number). Nevertheless, the cortical granules information of *A. turanica* and *A. ovalis* were not provided so far, the former can be separated from *A. sinica* sp. nov. by presence of contractile vacuole, higher numbers of adoral membranelles, cirri in ACR, and macronuclear nodules, and fewer dorsal

Table 3. Morphological comparison of eight *Amphisiella* species investigated using living observation and silver staining techniques.[a]

Character	*A. pulchra*	*A. sinica* sp. nov.	*A. annulata*	*A. capitata*[b]	*A. turanica*	*A. ovalis*[c]	*A. milnei*	*A. candida*
Body length in vivo	100–120	130–180	100–160	90–150	170–210	50–63	100–160	100–130
Body shape	Elongate elliptical, both cell ends rounded	Slender, fusiform anterior end narrowed	Slender and elongated, anterior end narrowed	Elongated with cephalised anterior region	Belt-like with both ends narrowed	Oval, posterior end broadly rounded	Elongate, both ends rounded	Elongate, both ends rounded
Contractile vacuole	Absent	Absent	Absent	Present	Present	–	Absent	Absent
Ring-shaped structures	Present	ca. 70–100 and densely arranged in both ends	Absent or several scattered distributed	Absent	Absent	–	Usually one each in cell end	Absent
Cortical granules	Colourless and grouped	Two types, bigger one globe-like, tiny one dot-like	Two types, bigger one globe-like, tiny one dot-like	Colourless globe-like, distribute along but not around dorsal bristle	–	–	Colourless, grouped in bands	Colourless, grouped in bands
No. of AZM	43–65	46–64	31–57	25–36	70–85	16–19	27–43	31–38
No. of cirri in ACR	49–64	41–52	25–54	31$\hat{5}$	ca. 67	18–22	22–36	23–31
No. of DK	7–9	6	6–8	5–6	4	4	7	5–7
No. of FC	3	3	3	3–5	3	2–4	4–6	3
PTC	Present	Present	Present	Absent	–	Present	Present	Present
No. of TC	5–7	6–7	5–6	6	6	6–7	4–5	4–5
No. of Ma	2	2	2	2	4	32–45	2	2
Data sources	Chen et al. (2013)	Present work	Berger (2004)	Li et al. (2007a)	Alekperov and Asadullayeva (1999)	Fernandez-Leborans and Novillo (2001)	Present work	Chen et al. (2013)

[a] All measurements in μm. ACR, amphisiellid median cirral row; AZM, adoral zone of membranelles; DK, dorsal kineties; FC, frontal cirri; Ma, macronuclear nodule; No., number; PTC, pretransverse ventral cirri; TC, transverse cirri.

"–" The characters were not provided in the source cited.

[b] Identified as *Amphisiella marioni*, which should be the junior synonym of *A. capitata.*

[c] The living characters are not clear from life, or after silver preparations.

kineties. In addition, *Amphisiella ovalis* differs from the new species in body shape (oval, posterior end broadly rounded in *A. ovalis* vs. slender fusiform with anterior end narrowed) and most of the morphometric data, inter alia, body size, numbers of adoral membranelles, dorsal kineties, cirri in amphisiellid medium cirral row, and macronuclear nodules (Alekperov and Asadullayeva 1999; Chen et al. 2013; Fernandez-Leborans and Novillo 1992, 2001; Li et al. 2007a).

As expected, the results of the molecular analysis, including the phylogenetic tree and similarity comparison using SSU rRNA gene sequences, are very consistent with the morphology and hence support the validity of *A. sinica* sp. nov. (Table 2; Fig. 7).

The phylogenetic position of two *Amphisiella* species

Amphisiella was considered to be a morphologically well-outlined and small assemblage (Berger 2004, 2008; Chen et al. 2013; Hu et al. 2004; Li et al. 2007a). It can be very easily separated from several other genera with an ACR by the lack of caudal cirri (presence in *Caudiamphisiella* Berger, 2004; *Protogastrostyla* Gong et al., 2007; *Hemiamphisiella* Foissner, 1988; *Trachelostyla* Borror, 1972; *Spiroamphisiella* Li, Song and Hu, 2007; and *Nudiamphisiella* Foissner, Agatha and Berger, 2002) (Berger 2008; Borror 1972; Foissner 1988; Gong et al. 2007; Li et al. 2007b; Shao et al. 2007). *Uroleptoides* Wenzel, 1953 morphologically differs from *Amphisiella* in the presence of a dorsomarginal row and kinety fragmentation (vs. absence in the latter) and habitat (terrestrial vs. saltwater) (Berger 2008; Foissner et al. 2002; Wenzel 1953).

However, the present molecular phylogenetic analyses could not get a consistent result with morphological classification. Five species with 18S rDNA sequence data available cluster into two isolated clades that contain three and two species respectively. Chen et al. (2013) demonstrated that *Amphisiella candida* clustered with all its congeners but with low support values (26% ML and not supported by BI), which means this relationship was unreliable. By contrast, our tree shows more reasonable topological relationships, based on careful identification with relatively high support values (ML 99% BI 1.00), among the target forms, which indicate that the genus *Amphisiella* is polyphyletic dividing into two distantly separated clades. Hereby, the conflict makes us to reconsider the true relationship among the *Amphisiella* species. The consistent common features of group I (*A. annulata* + *A. sinica* sp. nov. + *A. pulchra*), which are distinct from group II (*A. milnei* + *A. candida*) include: (1) the wide and narrowly spaced cirri of the ACR (vs. cirri within ACR of ordinary width and length, that is, not as wide, short, and narrowly spaced as in group I); (2) the anterior and posterior portion of the ACR is well pieced together to be a continuous row (vs. ACR is inconspicuously separated in group II); (3) one extra transverse cirrus is usually formed (vs. absence in group II); (4) the proximal portion of the adoral zone of membranelles is usually slightly spoon-shaped widened (vs. the adoral zone of membranelles are shaped like a normal question-mark) (Aladro-Lubel 1985; Aladro-Lubel et al. 1990; Berger 2004; Chen et al. 2013; Hu et al. 2004). Some minor differences are worth mentioning, but these should not be over-interpreted, inter alia: (1) the amphisiellid median cirral row posteriorly extends very close to the transverse cirri in group I, while a conspicuous gap is present between the posterior end of the ACR and the rear end of the body in group II; (2) the body shape is more or less cephalised in group I, while in group II the anterior body portion is not head-like (Berger 2004; Chen et al. 2013; Hu et al. 2004; Li et al. 2007a). These morphological and morphogenetic differences are not sufficient, however, to strongly support the splitting of the genus *Amphisiella* since infraciliature formation and SSU rRNA gene sequences are not available for all known *Amphisiella* species.

Acknowledgements

This work was supported by the National Natural Science Foundation of China (project numbers: 31430077, 41576134, 31172059) and the Laboratory for Marine Biology and Biotechnology, Qingdao National Laboratory for Marine Science and Technology, China. The authors extend their sincere appreciations to the Deanship of Scientific Research at King Saud University for its funding this prolific research group (PRG-1436-24).

References

Agamaliev, F.G., 1972. Ciliates from microbenthos of the islands of Apseronskij and Bakinskij archipelagos of the Caspian Sea. Acta Protozool. 10, 1–27 (in Russian with English summary).

Aladro-Lubel, M.A., 1985. Algunos ciliados intersticiales de Isla de Enmedio, Veracruz, México. An. Inst. Biol. Univ. Méx. Ser. Zool. 55 (1), 1–59 (1984) Lamina 1–17.

Aladro-Lubel, M.A., Martín-Murillo, M.E., Mayén-Estrado, R., Hernández-Anaya, M., Sánchez-Calderón, G., 1986. Cuarenta y nueve especies de ciliados intersticiales identificados en Boca del Río, Veracruz, México. Rev. Latam. Microbiol. 28, 231–242.

Aladro-Lubel, M.A., Martínez Murillo, M.E., Mayén Estrada, R., 1990. Manual de ciliados psamofilos marinos y salobres de Mexico. Cuadernos del Instituto de Biologia 9. Universidad Nacional Autonoma de Mexico, 174 pp.

Alekperov, I.K., Asadullayeva, E.S., 1999. New, little-known and characteristic ciliate species from the Apsheron coast of the Caspian Sea, Turkish. J. Zool. 23, 215–225.

Berger, H., 2004. Amphisiella annulata (Kahl, 1928) Borror, 1972 (Ciliophora: Hypotricha): morphology, notes on morphogenesis, review of literature, and neotypification. Acta Protozool. 43, 1–14.

Berger, H., 2008. Monograph of the Amphisiellidae and Trachelostylidae (Ciliophora, Hypotricha). Monogr. Biol. 88, 1–737.
Berger, H., Foissner, W., 1989. Morphology and biometry of some soil hypotrichs (Protozoa, Ciliophora) from Europe and Japan. Bull. Br. Mus. Nat. Hist. (Zool.) 55, 19–46.
Blatterer, H., Foissner, W., 1988. Beitrag zur terricolen Ciliatenfauna (Protozoa: Ciliophora) Australiens. Stapfia 17, 1–84.
Borror, A.C., 1963. Morphology and ecology of the benthic ciliated protozoa of Alligator Harbor, Florida. Arch. Protistenkd. 106, 465–534.
Borror, A.C., 1972. Revision of the order Hypotrichida (Ciliophora, Protozoa). J. Protozool. 19, 1–23.
Castresana, J., 2000. Selection of conserved blocks from multiple alignments for their use in phylogenetic analysis. Mol. Biol. Evol. 17, 540–552.
Chen, L., Zhao, X., Ma, H., Warren, A., Shao, C., Huang, J., 2015a. Morphology, morphogenesis and molecular phylogeny of a soil ciliate, *Pseudouroleptus caudatus caudatus* Hemberger, 1985 (Ciliophora, Hypotricha), from Lhalu wetland, Tibet. Eur. J. Protistol. 51, 1–14.
Chen, X., Shao, C., Lin, X., Clamp, J.C., Song, W., 2013. Morphology and molecular phylogeny of two new brackish-water species of *Amphisiella* (Ciliophora, Hypotrichia), with notes on morphogenesis. Eur. J. Protistol. 49, 453–466.
Chen, X., Gao, F., Al-Farraj, S.A., Al-Rasheid, K.A.S., Xu, K., Song, W., 2015b. Morphology and morphogenesis of a novel mangrove ciliate, *Sterkiella subtropica* sp. nov. (Protozoa, Ciliophora, Hypotrichia), with phylogenetic analyses based on small-subunit rDNA sequence data. Int. J. Syst. Microbiol. 65, 2292–2303.
Dragesco, J., 1963. Compléments a la connaissance des ciliés mésopsammiques de Roscoff. Cah. Biol. Mar. 4, 251–275.
Elwood, H.J., Olsen, G.J., Sogin, M.L., 1985. The small-subunit ribosomal RNA gene sequences from the hypotrichous ciliates *Oxytricha nova* and *Stylonychia pustulata*. Mol. Biol. Evol. 2, 399–410.
Fan, Y., Pan, Y., Huang, J., Hu, X., Lin, X., Warren, A., 2014. Molecular phylogeny and taxonomy of two novel brackish water hypotrich ciliates, with the establishment of a new genus, *Antiokeronopsis* gen. n. (Ciliophora, Hypotrichia). J. Eukaryot. Microbiol. 61, 449–462.
Fan, Y., Zhao, X., Hu, X., Miao, M., Warren, A., Song, W., 2015. Taxonomy and molecular phylogeny of two novel ciliates, with establishment of a new genus, *Pseudogastrostyla* n. g. (Ciliophora, Hypotrichia, Oxytrichidae). Eur. J. Protistol. 51, 374–385.
Fernandez-Leborans, G., Novillo, A., 1992. Morphology and taxonomy of two new species of marine ciliates (Ciliophora: Spirotrichea: Stichotrichida: Amphisiellidae). Proc. Boil. Soc. Wash. 105, 165–179.
Fernandez-Leborans, G., Novillo, A., 2001. A note about two hypotrich ciliate species of the genus *Amphisiella*. Acta Protozool. 40, 225–227.
Foissner, W., 1988. Gemeinsame Arten in der terricolen Ciliatenfauna (Protozoa: Ciliophora) von Australien und Afrika. Stapfia 17, 85–133.
Foissner, W., Agatha, S., Berger, H., 2002. Soil ciliates (Protozoa, Ciliophora) from Namibia (Southwest Africa), with emphasis on two contrasting environments, the Etosha region and the Namib desert. Part I: Text and line drawings. Part II: Photographs. Denisia 5, 1–1459.
Gong, J., Kim, S.J., Kim, S.Y., Min, G.S., Roberts, D.M., Warren, A., Choi, J.K., 2007. Taxonomic redescriptions of two ciliates, *Protogastrostyla pulchra* n. g., n. comb. and *Hemigastrostyla enigmatica* (Ciliophora: Spirotrichea, Stichotrichia), with phylogenetic analyses based on 18S and 28S rRNA gene sequences. J. Eukaryot. Microbiol. 54, 468–478.
Gourret, P., Roeser, P., 1888. Contribution à l'étude des protozoaires de la Corse. Arch. Biol. 8, 139–204, Planches XIII–XV.
Hall, T., 1999. BioEdit: a user-friendly biological sequence alignment editor and analysis program for Windows 95/98/NT. Nucleic Acids Symp. Ser. 41, 95–98.
Horváth, J., 1950. Contributions to studies on soil protozoa of the ciliata group, with special regard to their adaptation to soil conditions. Ann. Inst. Biol. Pervest Hung. 19, 151–162, 1949–1950.
Hu, X., Warren, A., Sudzuki, T., 2004. Morphology and morphogenesis of two marine ciliates, *Pseudokeronopsis pararubra* sp. n. and *Amphisiella annulata* from China and Japan (Protozoa: Ciliophora). Acta Protozool. 43, 351–368.
Jo, E., Jung, J.H., Min, G.S., 2015. Morphology and molecular phylogeny of two new brackish water ciliates of *Bakuella* (Ciliophora: Urostylida: Bakuellidae) from South Korea. J. Eukaryot. Microbiol. 62, 799–809.
Kahl, A., 1928. Die Infusorien (Ciliata) der Oldesloer Salzwasserstellen. Arch. Hydrobiol. 19, 50–123.
Kahl, A., 1932. Urtiere oder Protozoa. I: Wimpertiere oder Ciliata (Infusoria), 3. Spirotricha. Tierwelt Dtl. 25, 399–650.
Kahl, A., 1933. Ciliata libera et ectocommensalia. Tierwelt N.-u. Ostsee Lieferung 23 (Teil II. c3), 29–146.
Kumar, S., Nei, M., Dudley, J., Tamura, K., 2008. MEGA: A biologist-centric software for evolutionary analysis of DNA and protein sequences. Brief. Bioinform. 9, 299–306.
Li, J., Lin, X., Shao, C., Gong, J., Hu, X., Song, W., 2007a. Morphological redescription and neotypification of the marine ciliate, *Amphisiella marioni* Gourret & Roeser, 1888 (Ciliophora: Hypotrichida), a poorly known form misidentified for a long time. J. Eukaryot. Microbiol. 54, 364–370.
Li, L., Song, W., Hu, X., 2007b. Two marine hypotrichs and a new genus, *Spiroamphisiella* gen. nov. (Ciliophora, Hypotricha) from North China, with description of a new species *Spiroamphisiella hembergeri* spec. nov. Acta Protozool. 46, 107–120.
Lu, X., Gao, F., Shao, C., Hu, X., Warren, A., 2014. Morphology, morphogenesis and molecular phylogeny of a new marineciliate, *Trichototaxis marina* n. sp. (Ciliophora, Urostylida). Eur. J. Protistol. 50, 524–537.
Luo, X., Gao, F., Al-Rasheid, K.A.S., Warren, A., Hu, X., Song, W., 2015. Redefinition of the hypotrichous ciliate *Uncinata*, with descriptions of the morphology and phylogeny of three urostylids (Protista, Ciliophora). Syst. Biodivers. 13, 455–471.
Medlin, L., Elwood, H.J., Stickel, S., Sogin, M.L., 1988. The characterization of enzymatically amplified eukaryotic 16S-like rRNA-coding regions. Gene 71, 491–499.
Miller, M., Pfeiffer, W., Schwartz, T., 2010. Creating the CIPRES Science Gateway for inference of large phylogenetic trees. In: Proceedings of the Gateway Computing Environments Workshop (GCE), New Orleans, LA, pp. 1–8.
Nylander, J.A.A., 2004. MrModeltest, Version 2.0. Evolutionary Biology Centre. Uppsala University Press, Uppsala.
Penn, O., Privman, E., Ashkenazy, H., Landan, G., Graur, D., Pupko, T., 2010a. GUIDANCE: a web server for assessing alignment confidence scores. Nucleic Acids Res. 38, W23–W28.

Penn, O., Privman, E., Landan, G., Graur, D., Pupko, T., 2010b. An alignment confidence score capturing robustness to guide tree uncertainty. Mol. Biol. Evol. 27, 1759–1767.

Ronquist, F., Huelsenbeck, J., 2003. MRBAYES 3: Bayesian phylogenetic inference under mixed models. Bioinformatics 19, 1572–1574.

Shao, C., Song, W., Yi, Z., Gong, J., Li, J., Lin, X., 2007. Morphogenesis of the marine spirotrichous ciliate, *Trachelostyla pediculiformis* (Cohn, 1866) Borror, 1972 (Ciliophora, Stichotrichia), with consideration of its phylogenetic position. Eur. J. Protistol. 43, 255–264.

Song, W., Wilbert, N., 1997. Morphological investigations on some free living ciliates (Protozoa, Ciliophora) from China Sea with description of a new hypotrichous genus, *Hemigastrostyla* nov. gen. Arch. Protistenk. 148, 413–444.

Stamatakis, A., 2006. RAxML-VI-HPC: maximum likelihood-based phylogenetic analyses with thousands of taxa and mixed models. Bioinformatics 22, 2688–2690.

Stamatakis, A., Hoover, P., Rougemont, J., 2008. A rapid bootstrap algorithm for the RAxML web servers. Syst. Biol. 57, 758–771.

Wenzel, F., 1953. Die Ciliaten der Moosrasen trockner Standorte. Arch. Protistenk. 99, 70–141.

Wilbert, N., 1975. Eine verbesserte Technik der Protargolimprägnation für Ciliaten. Mikrokosmos 64, 171–179.

Wilbert, N., Song, W., 2005. New contributions to the marine benthic ciliates from the Antarctic area, including description of seven new species (Protozoa, Ciliophora). J. Nat. Hist. (Lond.) 39, 935–973.